forests

Article

Land-Cover and Elevation-Based Mapping of Aboveground Carbon in a Tropical Mixed-Shrub Forest Area in West Java, Indonesia

Elham Sumarga *, Nuruddin Nurudin and Ichsan Suwandhi

School of Life Sciences and Technology, Institut Teknologi Bandung, Jalan Ganesa 10, Bandung 40132, Indonesia; nurudin@sith.itb.ac.id (N.N.); ichsan@sith.itb.ac.id (I.S.)

* Correspondence: elham@sith.itb.ac.id; Tel.: +62-8131-208-2299

Received: 21 February 2020; Accepted: 20 May 2020; Published: 4 June 2020

Abstract: Carbon sequestration and storage are among the most important ecosystem services provided by tropical forests. Improving the accuracy of the carbon mapping of tropical forests has always been a challenge, particularly in countries and regions with limited resources, with limited funding to provide high-resolution and high-quality remote sensing data. This study aimed to examine the use of land-cover and elevation-based methods of aboveground carbon mapping in a tropical forest composed of shrubs and trees. We tested a geostatistical method with an ordinary kriging interpolation using three stratification types: no stratification, stratification based on elevation, and stratification based on land-cover type, and compared it with a simple mapping technique, i.e., a lookup table based on a combination of land cover and elevation. A regression modelling with land cover and elevation as predictors was also tested in this study. The best performance was shown by geostatistical interpolation without stratification and geostatistical interpolation based on land cover, with a coefficient of variation (CV) of the root mean square error (RMSE) of 0.44, better than the performance of lookup table techniques (with a CV of the RMSE of more than 0.48). The regression modeling provided a significant model, but with a coefficient of determination (R^2) of only 0.29, and a CV of the RMSE of 0.49. The use of other variables should thus be further investigated. We discuss improving aboveground carbon mapping in the study area and the implications of our results for forest management.

Keywords: aboveground biomass; geostatistics; kriging; regression modeling; stratification; tropical forest

1. Introduction

The concept of ecosystem services has been widely used to analyze the contribution of ecosystems to society [1]. Tropical forests provide different types of ecosystem services, prominent among them being climate regulation, particularly in the form of carbon sequestration and storage [2,3]. Currently, there is global concern regarding this service because of increasing carbon accumulation in the atmosphere, particularly of carbon dioxide (CO_2) [4], which is one of the main greenhouse gases [5].

Mapping carbon storage in tropical forests is an effective way of elucidating how much carbon is stored in forests and its spatial distribution. This information is particularly important for protected forests, where optimizing ecosystem function is an important management objective [6], including optimizing carbon sequestration and storage. Different methods have been developed to map carbon storage in tropical forests, which, in general, can be classified as non-remote and remote sensing methods. Non-remote sensing methods only use ground measurement data as the basis for mapping, with the application of various interpolation techniques as the common mapping method (e.g., [7]).

Remote sensing methods are more advanced and combine ground measurement data with a wide range of both optical and microwave remote sensing data (e.g., [8,9]). The latter methods include a simple lookup table method that links ground measurement data to a land-cover map that is generated from satellite image classification (e.g., [10]), regression model development using different spectral variables and indices derived from satellite image data as predictors (e.g., [11,12]), a combination of regression modeling and kriging interpolation (e.g., [13]), and the application of LiDAR (light detection and ranging) (e.g., [14,15]) and RADAR (radio detection and ranging) (e.g., [16]) data. Developing an efficient method with an acceptable level of accuracy is a considerable challenge, particularly in countries and regions with limited resources, with limited access to high-resolution and high-quality remote sensing data.

There is a common trade-off between mapping accuracy and feasibility. Achieving a good mapping accuracy is often constrained by several limitations, including budget, in regard to the implementation of a mapping technique [17]. The use of some remote sensing data such as LiDAR and high-resolution optical and RADAR data, despite their capability in well mapping the aboveground carbon of forest [18,19], are too expensive for a periodic mapping of the aboveground carbon of forest in many regions in developing countries. In regard to this issue, the potential use of some free remote sensing data for the aboveground carbon mapping of forest needs to be further investigated. This includes the wide possibility of the use of land-cover and elevation data generated from freely accessible remote sensing data, such as Google Earth and Shuttle Radar Topography Mission (SRTM) data.

This study aimed to examine the use of some land-cover and elevation-based mapping techniques to map aboveground carbon in a tropical mixed-shrub forest area, with a case study in the Mount Geulis forest, Indonesia. The tropical forest on Mount Geulis is composed of plantations and natural vegetation. The area has been designated as a protected forest, with an additional function as an educational forest. As a protected forest, Geulis Mountain is managed to optimize the provision of different types of ecosystem services. To this end, the diversity of the ecosystem services provided by the forest should be properly identified, quantified, and mapped, including for the carbon storage service.

This study concerns testing the performance of some relatively low-cost methods of aboveground carbon mapping that are potentially applied for tropical forest with an area of less than 500 hectares. We integrated field measurement to obtain carbon data and the use of free remote sensing data to generate land-cover and elevation data. We used the land cover and elevation as the basis for aboveground carbon mapping with three different techniques, i.e., geostatistical interpolation, regression modeling, and the lookup table. The three mapping techniques have different characteristics in terms of spatial modeling and in terms of the way land cover and elevation are integrated in the modeling. The geostatistical interpolation uses the spatial autocorrelation among sampled aboveground carbon data as the basis for prediction, which in this study was performed in three different stratifications, i.e., no stratification, stratification based on land cover, and stratification based on elevation classes. The regression modeling directly models the relationship between sampled aboveground carbon data (as response variables) and land cover and elevation (as predictors), and applies the model to predict the aboveground carbon in unsampled locations. The lookup table simply calculates the average values of above ground carbon in each land cover and elevation class, and uses the values to map the aboveground carbon in the study area. This study analyzes the performance of the three mapping techniques, as an attempt to find an effective method of aboveground carbon mapping that could potentially be applied across a wider region.

2. Materials and Methods

2.1. Study Area

The Geulis Mountain forest is a protected forest in the middle of West Java province, Indonesia (107.794–107.814 E and 6.922–6.947 S). The Geulis Mountain forest covers 338 hectares with elevation that ranges from 800 to 1250 m above sea level. The land-cover map of the area (Figure 1) was generated based on the classification of Google Map images 2017, by combining visual interpretation and the ground survey data of land-cover types. The image consists of three bands (red, green, and blue), with a spatial resolution of 1.2 m. There is no spectral information of the image. However, with the mentioned spatial resolution, objects are clearly identified, and it allows visual interpretation for the land cover classification. The classification was performed by on-screen digitizing, using 95 samples of ground data of land cover as the inputs.

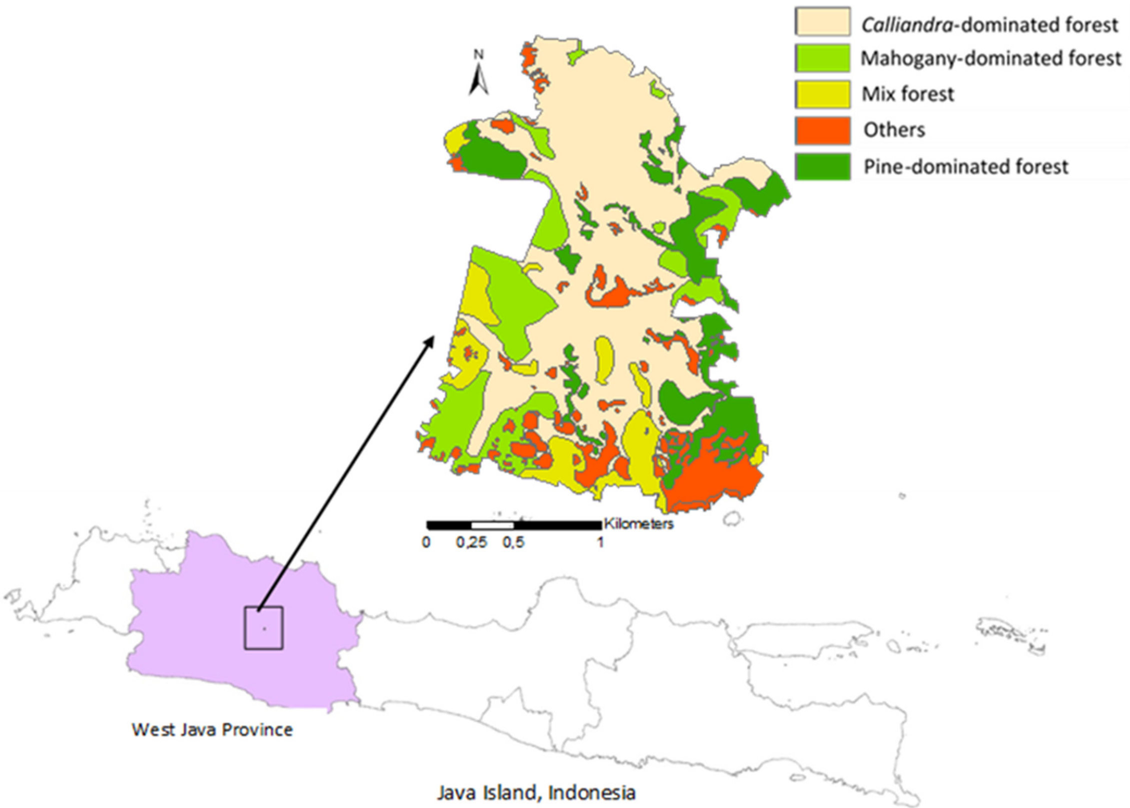

Figure 1. Geographical location and land-cover types of the Geulis Mountain forest.

2.2. Sampling Method

In total, 95 plots were sampled in a systematic way by considering the variation in elevation (Figure 2). The plots consisted of three squares, i.e., 20 × 20 m for tree measurement, 10 × 10 m for pole measurement, and 5 × 5 m for sapling measurement. The main data collected in each plot were the tree species and diameter at breast height (DBH), which were used to estimate the aboveground carbon using an allometric equation. The field data collection was performed in August–September 2017.

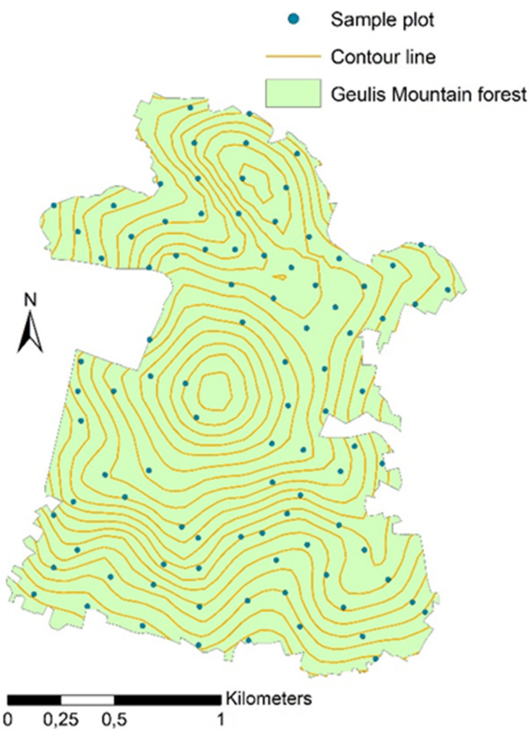

Figure 2. Distribution of sample plots.

2.3. Aboveground Carbon Estimation

The aboveground carbon in each plot was calculated using four types of allometric equation (Table 1), based on the tree species. The equations converted tree dbh into aboveground biomass. Pine (*Pinus merkusii*) and mahogany (*Swietenia macrophylla*) are the dominant tree species on the lower part of the mountain, while *Calliandra calothyrsus* covers about 49% of the area. Allometric equations were available for the three species. For other tree species, an equation from Ketterings et al. [20] for tropical trees in general was used. We realize that the use of allometric equations, particularly a general allometric equation, becomes a source of error in aboveground carbon estimation, which, subsequently, will potentially propagate in aboveground mapping. We further discuss this aspect in the Discussion section. We used a ratio of 0.47 for the conversion of aboveground biomass into aboveground carbon [21].

Table 1. Allometric equations used for converting the diameter at breast height into aboveground biomass.

Tree Species	Allometric Equations	Sources
Pine (*Pinus merkusii*)	$B = 0.066\ D^{2.51}$	Sya'bani [22].
Mahogany (*Swietenia macrophylla*)	$B = 0.048\ D^{2.68}$	Adinugroho and Sidiyasa [23].
Calliandra calothyrsus	$B = 0.047\ D^{2.493}$	Alhamd and Rahajoe [24].
Other tree species	$B = 0.066\ D^{2.59}$	Ketterings et al. [20].

B: aboveground biomass (kg); D: diameter at breast height (cm).

2.4. Mapping Methods and Validation

We applied three mapping techniques for aboveground carbon mapping, i.e., geostatistical interpolation, regression modeling, and the lookup table, using land cover and elevation as key factors. The elevation data was generated from the Digital Elevation Model (DEM) of the SRTM. From the 95 sampled data, we randomly selected 80% of the data for the inputs of modeling and mapping, and allocated the rest (20% of the data) for validation. In this way, the performance of the three mapping techniques was validated in the same way using independent validation data. The accuracy of the mapping techniques was checked by calculating the overall coefficient of variation (CV) of the root mean square error (RMSE) [25] using the independent validation data. This coefficient represents the deviation of the prediction error from the mean of the validation data. The lowest value is 0, where a CV of the RMSE of 0 indicates perfect accuracy. The procedures of the three mapping techniques are described in Sections 2.4.1–2.4.3.

2.4.1. Lookup Table

The lookup table can be considered as the simplest technique to map aboveground carbon. This technique assumes a uniform distribution of aboveground carbon in all areas (pixels) within the same class. We used land-cover type and a combination of land-cover type and elevation as the basis for classification. The estimate of aboveground carbon in each class was the mean amount of carbon in that class, selected from the training sample data. Hence, we have five variations of aboveground carbon values in mapping using a lookup table based on land cover, and 10 variations in mapping using a lookup table based on a combination of land-cover and elevation classes.

2.4.2. Regression Modeling

We used linear regression modeling to map aboveground carbon using information on land cover and elevation as the explanatory variables. We extracted the type of land cover and the value of elevation in all training sampled points of aboveground biomass measurement and ran a linear regression modeling in the "R" statistical software [26]. We then analyzed the significance of the explanatory variables in determining the values of aboveground carbon. In order to map the distribution of the aboveground carbon, we applied the regression model in a spatial analysis using a raster calculator tool of ArcGIS 10.5. In addition to calculating the CV of the RMSE, the accuracy of the regression model was also analyzed by the coefficient of determination (R^2).

2.4.3. Geostatistical Interpolation

We applied the geostatistical method to model the spatial structure of the training aboveground carbon data using variogram analysis in the "R" statistical software. This analysis requires that the data are normally distributed; hence, at the first step we checked the distribution of the aboveground carbon data. Since the data were not normally distributed, we converted the data into log data, and found that the log data had a more normal distribution. We then used the log data for further variogram analysis. This analysis investigated the spatial autocorrelation among the log of the aboveground carbon data. Ideally, when spatial autocorrelations among data are significant, nearby locations tend to have similar values (low variance).

A gstat library [27] was used for variogram analysis, which selected the best variogram model. The parameters of the best variogram model (partial sill, range, and nugget) were then used in an ordinary kriging interpolation. Since we used the log of aboveground carbon data in variogram modeling, this required us to revert back the predicted values into aboveground carbon, and we presented them in an aboveground carbon map.

To see the possibility to enhance the accuracy of the geostatistical interpolation, we did a stratified geostatistical analysis, using land cover and elevation as the basis for stratification. Hence, the geostatistical analysis in this study was applied for three stratification types: no stratification, stratification based on elevation, and stratification based on land-cover type. We used two elevation classes (>1025 m and <1025 m) and five land-cover types: pine-dominated forest, mahogany dominated forest, *Calliandra*-dominated shrubs, mixed forest, and other types.

3. Results

From field observations in 95 sampled plots, this study identified 52 different tree species, including a woody shrub dominating the study area, i.e., *Calliandra calothyrsus*. Other dominant trees include *Swietenia macrophylla*, *Pinus merkusii*, *Toona sinensis*, *Maesopsis eminii*, *Paraserianthes falcataria*, and *Hibiscus macrophyllus*. By using the available allometric equations, the aboveground carbon of each stand was calculated, and subsequently, the aboveground carbon of all stands in a plot was combined to estimate the aboveground carbon of each plot. We found a large variation in the amount of aboveground carbon in the different land cover types (Table 2). The aboveground carbon ranged from 1.3 ton C/ha to 165.1 ton C/ha, with an average of 33.5 ton C/ha. The original data of aboveground carbon in all 95 sampled plots, together with the related information on elevation and land cover, is presented in Appendix A.

Table 2. Range, mean, and standard deviation of aboveground carbon in different land cover types in the Geulis Mountain forest.

Land Cover Types	Number of Plots	Range (ton C/ha)	Mean (ton C/ha)	Standard Deviation (ton C/ha)	Standard Error (ton C/ha)	Relative Standard Error (%)
Pine-dominated forest	11	3.8–101.5	42.5	29.0	8.7	21
Mahogany-dominated forest	17	11.1–165.1	72.5	36.3	8.8	12
Calliandra-dominated shrubs	43	3.8–142.1	26.5	25.9	4.0	15
Mixed forest	13	16.8–107.2	59.5	29.5	8.2	14
Others	11	1.3–98.0	25.0	27.7	8.4	33

To find an efficient way to map the distribution of the aboveground carbon with an appropriate accuracy, we tested six mapping techniques, involving geostatistical interpolation, regression modeling, and a lookup table, using land cover and elevation as the basis for stratification and prediction. The performance of each mapping technique is described in Sections 3.1–3.6.

3.1. Lookup Table Based on Land Cover

Figure 3a shows an aboveground carbon map resulting from the lookup table technique based on land-cover type. This mapping technique ignores variation in the aboveground carbon data from locations with the same type of land cover. The map only shows variation in the aboveground carbon between different land-cover types, using the means of the training data as predicted values for each land-cover type, as listed in Table 3. The result of validation showed that this technique provided a moderate accuracy with a CV of the RMSE of 0.48.

Table 3. Mean values of above ground carbon used for the lookup table mapping.

Types of Lookup Table	Classes	Mean Aboveground Carbon (ton C/ha)
Based on land-cover types	Pine-dominated forest	44.4
	Mahogany-dominated forest	72.8
	Calliandra-dominated shrubs	27.3
	Mixed forest	57.4
	Others	27.3

Table 3. *Cont.*

Types of Lookup Table	Classes	Mean Aboveground Carbon (ton C/ha)
Based on a combination of elevation and land-cover types	Pine-dominated forest, high elevation	16.6
	Pine-dominated forest, low elevation	47.5
	Mahogany-dominated forest, high elevation	61.1
	Mahogany-dominated forest, low elevation	93.1
	Calliandra-dominated shrubs, high elevation	23.4
	Calliandra-dominated shrubs, low elevation	32.9
	Mixed forest, high elevation	59.4
	Mixed forest, low elevation	56.6
	Others, high elevation	35.3
	Others, low elevation	26.4

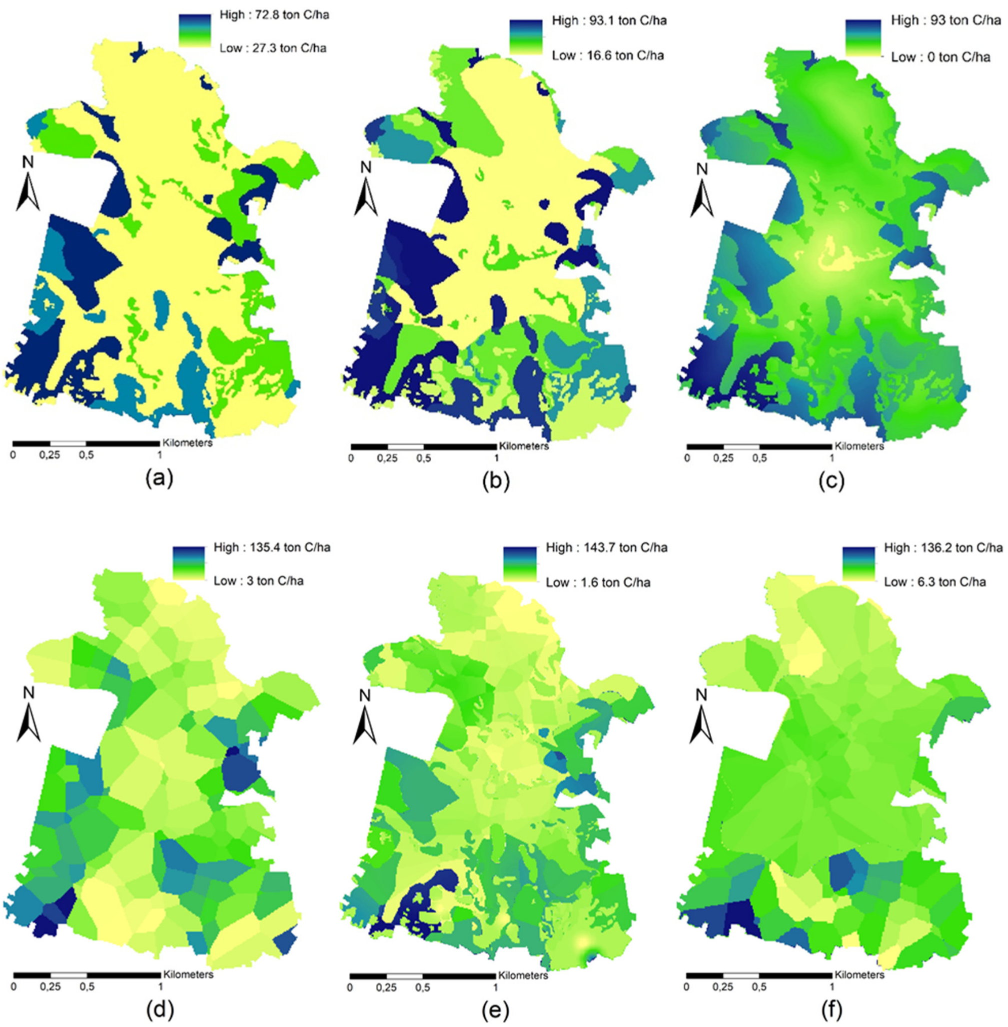

Figure 3. Maps of aboveground carbon in the Geulis Mountain forest generated from the following. (**a**) Lookup table based on land-cover type; (**b**) Lookup table based on a combination of land cover and elevation; (**c**) Regression modeling; (**d**) Geostatistical interpolation without stratification; (**e**) Stratified geostatistical interpolation based on land-cover type; (**f**) Stratified geostatistical interpolation based on elevation.

3.2. Lookup Table Based on a Combination of Land Cover and Elevation

Figure 3b shows an aboveground carbon map resulting from a lookup table technique based on a combination of land-cover type and elevation. The mean values of aboveground carbon in each combination used in this mapping are listed in Table 3. Combining elevation classes with land-cover types makes a more detailed unit for mapping, so it was expected that this technique would have a lower mapping error. However, the result of validation showed that this technique did not perform better than the lookup table technique that only considered land-cover type, with a CV of the RMSE of 0.49.

3.3. Regression Modeling

Table 4 summarizes the results of the regression modeling of the aboveground carbon using land cover and elevation as predictors. Both land cover and elevation are significant in explaining the variation of the aboveground carbon in the Geulis Mountain forest. Elevation has a negative relationship with aboveground carbon, where higher elevation tends to have a smaller amount of aboveground carbon. In terms of land cover, the regression took *Calliandra*-dominated shrubs as the baseline. Compared to the baseline land cover, only one land cover type was shown to present a significantly higher amount of aboveground carbon, i.e., mahogany dominated forest (p value less than 0.01). The coefficient of determination (R^2) of the regression model is 0.29, indicating that about 71% of the variation of the aboveground carbon in the Geulis Mountain forest could not be explained by the model. Figure 3c presents the map of aboveground carbon in the Geulis Mountain forest generated from the regression model. Based on validation using independent data, this technique provided a moderate accuracy, with a CV of the RMSE of 0.49.

Table 4. Summary of the results of regression modeling.

Variables	Coefficients	p Values
Intercept	120,329.49	0.0108 *
Elevation	−88.59	0.0452 *
Land cover (mahogany-dominated forest)	40,906.18	0.0003 **
Land cover (mix forest)	21,717.33	0.0583
Land cover (pine-dominated forest)	9397.80	0.4181
Land cover (others)	−10,497.10	0.3867

Note: the unit of aboveground carbon is in kg/ha; * significant at an α of 0.05; ** significant at an α of 0.01.

3.4. Geostatistical Interpolation without Stratification

Table 5 presents the accuracy measure (CV of the RMSE) from the validation of the geostatistical interpolation of aboveground carbon data using three stratification types: no stratification, stratification based on land cover, and stratification based on elevation. With a CV of the RMSE of 0.44, the geostatistical interpolation without stratification can be considered to have a moderate accuracy. Figure 3d shows the aboveground carbon map of the Geulis Mountain forest generated from geostatistical interpolation without stratification.

Table 5. Coefficients of variation (CVs) of the root mean square error (RMSE) of the geostatistical interpolation of aboveground carbon in the Geulis Mountain forest.

Geostatistical Interpolation Technique	Strata	CV of RMSE	Overall CV of RMSE
Geostatistical interpolation without stratification	No strata	0.44	0.44
Geostatistical interpolation based on land cover	Pine-dominated forest	0.26	0.44
	Mahogany-dominated forest	0.35	
	Calliandra-dominated shrubs	0.52	
	Mixed forest	0.48	
	Other types	0.34	
Geostatistical interpolation based on elevation	High elevation (>1025 m)	0.46	0.56
	Low elevation (<1025 m)	0.57	

3.5. Stratified Geostatistical Interpolation Based on Land Cover

The purpose of stratification is to reduce variation among sampling data, because areas on the same stratum usually provide similar data. Figure 3e shows an aboveground carbon map of the Geulis Mountain forest generated from stratified geostatistical interpolation, with land-cover type as the basis for stratification. Validation showed that a better accuracy of interpolation was achieved in pine-dominated areas, mahogany-dominated areas, and other types areas. However, overall, this technique was not capable of improving the accuracy of mapping compared to the geostatistical interpolation without stratification, with the same value of CV of the RMSE (from five land-cover types) of 0.44.

3.6. Stratified Geostatistical Interpolation Based on Elevation

Classifying aboveground carbon data based on elevation is another method of reducing variation in the data. However, the results of validation showed that this technique even provided worse accuracy in mapping aboveground carbon compared to the geostatistical interpolation without stratification, indicated by an overall CV of the RMSE of 0.56 (Table 2). The map of aboveground carbon resulting from geostatistical interpolation based on land cover is presented in Figure 3f.

4. Discussion

This study has shown the application of several land cover and elevation-based mapping methods, with relatively low implementation costs. Among the six mapping techniques examined, this study found that two geostatistical interpolations, i.e., geostatistical interpolation without stratification and geostatistical interpolation based on land cover, provided the lowest error in mapping aboveground carbon in the Geulis Mountain forest, with a CV of the RMSE of 0.44. Previous studies have found that some geostatistical applications for mapping aboveground forest biomass (or carbon) performed well. For example, Scolforo et al. [7] examined three geostatistical interpolation techniques to map the carbon stock of arboreal vegetation in the Brazilian biomes of the Atlantic Forest and Savanna: ordinary kriging, co-kriging, and regression kriging, and found that regression kriging performed best, with an agreement index (Willmott index) of 0.67. Li et al. [28] applied geostatistical modeling by integrating airborne LiDAR and SPOT−6 data to map aboveground biomass in a temperate forest in northeast China, and reported that two geostatistical interpolation methods performed well, i.e., ordinary kriging and regression kriging, with R^2 values of 0.6 and 0.67, respectively. This study suggests the application of this technique for aboveground carbon mapping in wider regions with roughly similar conditions, i.e., in tropical forests with areas of less than 500 hectares in developing countries, particularly in areas managed as protected forest with similar land cover composition.

This study also identified the potential application of regression modeling for aboveground carbon mapping using land cover and elevation as predictor variables, although more efforts are required. Elevation and one land cover type (mahogany-dominated forest) are significant in explaining the variation of aboveground carbon, but their contribution is only about 29%. This means that about 71%

of the variation of the aboveground carbon can be explained by other variables, which are unknown in the context of this study. Hence, this study suggests to examine the use of other variables that are potentially capable of improving the accuracy of mapping. With the development of low-cost methods for aboveground carbon mapping still the main concern, we suggest to further examine several variables that can be generated from free DEM and satellite images such as slope, aspect, and vegetation indices. Incorporating the non-remote sensing-based variables, particularly the ones that are critical for plant growth such as soil and geology, will also be a potential option for the accuracy improvement. Of course, this requires the availability of spatial data of the variables to allow the use of the variables in the regression modeling and aboveground carbon mapping.

We also refer another potential way of improving the accuracy of carbon mapping, i.e., developing allometric equations for more tree species. The aboveground biomass of most of the trees in the study area was calculated using a general allometric equation, which probably produced a high estimation error. This relates to the fact that different tree species commonly have different characteristics of wood density, hence each species ideally should have its own model that relates its DBH to aboveground biomass. Since the estimated values of the aboveground carbon in the sampled locations were then used as the basis for modeling, this implies the further distribution of the error in estimating the aboveground carbon in unsampled locations. For certain, we cannot ensure that this error was directly related to the high mapping error. Hence, whether improving the accuracy of aboveground carbon estimation is capable of improving the accuracy of aboveground carbon mapping should be further investigated.

Many studies have reported that protected areas are characterized by high variability and a large number of ecosystem services [29,30], which can be used as indicators of the success of forest management. In this context, this study has made an important contribution in providing data on ecosystem services, because carbon storage is one of the key forest ecosystem services. Based on the best mapping technique examined in this study, the estimate of the total aboveground carbon in the study area is about 10,410 tons, with an average value of 30.8 ton C/ha. This value is comparable to the aboveground carbon of several plantation forests in West Java Province, e.g., *Acacia mangium* forest (28 ton C/ha) and *Anthocephalus cadamba* forest (31.5 ton C/ha) [31]. However, the value is much lower compared to the aboveground carbon of Indonesian natural dryland forest, both the primary forest (about 234 ton C/ha [32]) and the secondary forest with a low degradation level (about 148 ton C/ha [33] or 150 ton C/ha [34]). This is related to the vegetation types of the Geulis Mountain forest, which is composed of plantation trees and naturally growing shrubs. Please note that in terms of providing information on carbon storage, the total carbon storage of a forest is actually composed of aboveground carbon, belowground carbon (carbon stored in roots), soil carbon, and carbon stored in deadwood and litter. Since this study focused on mapping aboveground carbon, further analysis is required to reveal the total carbon stored in the forest. For this purpose, the results of this study can be used as a basis for estimating another part of carbon storage, particularly the belowground carbon, using, for example, the root to shoot ratio [35] as an approach.

Another potential use of aboveground carbon maps in support of forest management is in providing input for spatial planning, including for fire risk management. Fires frequently take place in the Geulis Mountain forest, particularly in the dry season. This disturbance can be related to the occasional use of fire for agricultural practices around the forest, usually for land clearance, as in 2018. This is quite common in the context of Indonesian forest fires, which can be strongly linked to human activity [36,37]. The availability of an aboveground carbon map, combined with burn severity information, can be useful to estimate the loss of aboveground carbon from forest fires [38], and further to identify high-priority sites for fire prevention. In a more general applications, many studies have successfully demonstrated the use of spatial information about multiple ecosystem services, including carbon sequestration and storage, in the support of land-use planning at different levels of land-use management [39–41].

5. Conclusions

The aboveground carbon measured in the tropical forest of the Mount Geulis, in West Java (Indonesia), ranged from 1.3 ton C/ha to 165.1 ton C/ha, with an average of 33.5 ton C/ha. Among the six mapping techniques considered, the highest accuracy was achieved using geostatistical interpolation without stratification and geostatistical interpolation based on land cover, with a CV of the RMSE of 0.44. Aboveground carbon mapping using stratification based on elevation was incapable of improving the accuracy of geostatistical interpolation. The computed validation statistics showed that this method was even outperformed by the methods of regression modeling, a lookup table based on land cover, and a lookup table based on a combination of land cover and elevation. There are several ways of improving the accuracy of carbon mapping in the study area, including testing the significance of other variables in regression modeling, developing specific allometric equations for more tree species, and expanding carbon mapping to other ecosystem components (carbon in the roots, soil, dead wood, and litter). These methodologies may be tested in regions with limited resources, without high-quality and expensive remote sensing data.

Author Contributions: Conceptualization, E.S.; methodology, E.S., N.N., I.S.; software, E.S.; validation, E.S., N.N., I.S.; formal analysis, E.S., N.N., I.S.; investigation, E.S., N.N., I.S.; resources, E.S., N.N., I.S.; data curation, E.S., N.N., I.S.; writing—original draft preparation, E.S.; writing—review and editing, E.S.; visualization, E.S.; supervision, E.S.; project administration, E.S.; funding acquisition, E.S., N.N., I.S. All authors have read and agreed to the published version of the manuscript.

Funding: This research was funded by the Institute for Research and Community Services Institut Teknologi Bandung, and was partially funded by the Indonesian Ministry of Research and Technology, and the Indonesian Ministry of Education and Culture under World Class University (WCU) Program managed by Institut Teknologi Bandung.

Acknowledgments: We thank Agus Muhamad Maulana and his team for their kind support during field observation. We also thank two anonymous reviewers for their comments and suggestions.

Conflicts of Interest: The authors declare no conflict of interest. The funders had no role in the design of the study; in the collection, analyses, or interpretation of data; in the writing of the manuscript, or in the decision to publish the results.

Appendix A

Table A1. Aboveground carbon data from 95 sampled plots in the Geulis Mountain forest.

Plot no	Aboveground Carbon (ton C/ha)	Land Cover Types	Elevation (Meter above Mean Sea Level)
1	98.0	Others	836
2	87.4	Mix forest	853
3	61.9	Mix forest	810
4	1.3	Others	904
5	15.1	Others	824
6	107.2	Mix forest	815
7	19.2	Mix forest	903
8	31.6	Others	938
9	31.6	Pine-dominated forest	938
10	2.5	Others	907
11	165.1	Mahogany-dominated forest	808
12	75.0	Pine-dominated forest	936
13	3.9	Others	877

Table A1. *Cont.*

Plot no	Aboveground Carbon (ton C/ha)	Land Cover Types	Elevation (Meter above Mean Sea Level)
14	111.1	Mahogany-dominated forest	803
15	77.7	Mix forest	850
16	3.8	Others	897
17	32.4	Pine-dominated forest	990
18	87.8	Mahogany-dominated forest	853
19	22.2	Pine-dominated forest	890
20	22.5	Others	1010
21	49.3	Mahogany-dominated forest	895
22	7.6	*Calliandra*-dominated shrub	983
23	32.8	Mix forest	908
24	56.6	*Calliandra*-dominated shrub	957
25	70.3	Mahogany-dominated forest	956
26	101.5	Pine-dominated forest	907
27	15.5	*Calliandra*-dominated shrub	1056
28	62.1	*Calliandra*-dominated shrub	981
29	142.1	*Calliandra*-dominated shrub	965
30	11.8	*Calliandra*-dominated shrub	1067
31	40.1	*Calliandra*-dominated shrub	986
32	35.8	Mix forest	918
33	40.6	Mix forest	998
34	52.1	Mix forest	994
35	64.3	Mix forest	1079
36	29.8	*Calliandra*-dominated shrub	1024
37	45.4	*Calliandra*-dominated shrub	1088
38	37.1	*Calliandra*-dominated shrub	1072
39	35.3	*Calliandra*-dominated shrub	1092
40	35.3	Others	1092
41	33.9	*Calliandra*-dominated shrub	1097
42	25.2	Others	1016
43	27.4	*Calliandra*-dominated shrub	1123
44	17.7	*Calliandra*-dominated shrub	1045
45	9.9	*Calliandra*-dominated shrub	1169
46	80.9	Mix forest	992
47	33.1	*Calliandra*-dominated shrub	1246
48	71.6	Mahogany-dominated forest	1103
49	19.1	*Calliandra*-dominated shrub	1160
50	16.8	Mix forest	1040
51	56.7	Mahogany-dominated forest	1102
52	107.7	Mahogany-dominated forest	1021
53	3.8	*Calliandra*-dominated shrub	1196
54	97.2	Mix forest	1145
55	74.5	Mahogany-dominated forest	1090

Table A1. *Cont.*

Plot no	Aboveground Carbon (ton C/ha)	Land Cover Types	Elevation (Meter above Mean Sea Level)
56	6.2	*Calliandra*-dominated shrub	1143
57	90.1	Mahogany-dominated forest	1048
58	54.3	Mahogany-dominated forest	1089
59	100.8	Mahogany-dominated forest	1070
60	19.4	*Calliandra*-dominated shrub	1136
61	57.2	Mahogany-dominated forest	1063
62	45.3	*Calliandra*-dominated shrub	1078
63	64.0	Pine-dominated forest	1004
64	24.8	*Calliandra*-dominated shrub	1066
65	57.7	Pine-dominated forest	1015
66	54.8	Mahogany dominated forest	1087
67	4.1	*Calliandra*-dominated shrub	1069
68	18.5	*Calliandra*-dominated shrub	1054
69	24.0	*Calliandra*-dominated shrub	1074
70	25.0	Mahogany dominated forest	1004
71	23.6	*Calliandra*-dominated shrub	1031
72	4.5	*Calliandra*-dominated shrub	1067
73	23.5	Pine-dominated forest	910
74	95.5	*Calliandra*-dominated shrub	1054
75	27.5	*Calliandra*-dominated shrub	1023
76	6.9	*Calliandra*-dominated shrub	1015
77	35.8	*Calliandra*-dominated shrub	964
78	17.9	*Calliandra*-dominated shrub	978
79	16.6	Pine-dominated forest	1086
80	39.5	Pine-dominated forest	964
81	3.8	Pine-dominated forest	850
82	45.5	Mahogany-dominated forest	954
83	6.3	*Calliandra*-dominated shrub	1130
84	5.6	*Calliandra*-dominated shrub	940
85	30.8	*Calliandra*-dominated shrub	1051
86	36.2	Others	895
87	7.4	*Calliandra*-dominated shrub	1117
88	16.7	*Calliandra*-dominated shrub	899
89	14.2	*Calliandra*-dominated shrub	993
90	12.9	*Calliandra*-dominated shrub	1147
91	11.1	*Calliandra*-dominated shrub	1035
92	41.1	*Calliandra*-dominated shrub	1039
93	5.5	*Calliandra*-dominated shrub	1094
94	4.5	*Calliandra*-dominated shrub	998
95	12.5	*Calliandra*-dominated shrub	954

References

1. United Nations; European Commissions; Food and Agriculture Organization of the United Nations; International Monetary Fund; Organisation for Economic Co-operation and Development; The World Bank. *System of Environmental-Economic Accounting 2012 Central Framework*; United Nations: New York, NY, USA, 2014.
2. Shimamoto, C.Y.; Botosso, P.; Marques, M.C.M. How much carbon is sequestered during the restoration of tropical forests? Estimates from tree species in the Brazilian Atlantic forest. *For. Ecol. Manag.* **2014**, *329*, 1–9. [CrossRef]
3. Wheeler, C.E.; Omeja, P.A.; Chapman, C.A.; Glipin, M.; Tumwesigye, C.; Lewis, S.L. Carbon sequestration and biodiversity following 18 years of active tropical forest restoration. *For. Ecol. Manag.* **2016**, *373*, 44–55. [CrossRef]
4. Fernández-Amador, O.; Francois, J.F.; Tomberger, P. Carbon dioxide emissions and international trade at the turn of the millennium. *Ecol. Econ.* **2016**, *125*, 14–26. [CrossRef]
5. Putman, W.M.; Ott, L.; Darmenov, A.; da Silva, A. A global perspective of atmospheric carbon dioxide concentrations. *Parallel Comput.* **2016**, *55*, 2–8. [CrossRef]
6. Hummel, C.; Poursanidis, D.; Orenstein, D.; Elliott, M.; Adamescu, M.C.; Cazacu, C.; Ziv, G.; Chrysoulakis, N.; van der Meer, J.; Hummel, H. Protected Area management: Fusion and confusion with the ecosystem services approach. *Sci. Total Environ.* **2019**, *651*, 2432–2443. [CrossRef] [PubMed]
7. Scolforo, H.F.; Scolforo, J.R.S.; de Mello, J.M.; de Mello, C.R.; Morais, V.A. Spatial interpolators for improving the mapping of carbon stock of the arboreal vegetation in Brazilian biomes of Atlantic forest and Savanna. *For. Ecol. Manag.* **2016**, *376*, 24–35. [CrossRef]
8. Shen, W.; Li, M.; Huang, C.; Tao, X.; Wei, A. Annual forest aboveground biomass changes mapped using ICESat/GLAS measurements, historical inventory data, and time-series optical and radar imagery for Guangdong province, China. *Agric. For. Meteorol.* **2018**, *259*, 23–38. [CrossRef]
9. Fayad, I.; Baghdadi, N.; Guitet, S.; Bailly, J.S.; Hérault, B.; Gond, V.; El Hajj, M.; Minh, D.H.T. Aboveground biomass mapping in French Guiana by combining remote sensing, forest inventories and environmental data. *Int. J. Appl. Earth Obs. Geoinf.* **2016**, *52*, 502–514. [CrossRef]
10. Temgoua, L.F.; Momo Solefack, M.C.; Nguimdo Voufo, V.; Tagne Belibi, C.; Tanougong, A. Spatial and temporal dynamic of land-cover/land-use and carbon stocks in Eastern Cameroon: A case study of the teaching and research forest of the University of Dschang. *For. Sci. Technol.* **2018**, *14*, 181–191. [CrossRef]
11. Zhu, J.; Huang, Z.; Sun, H.; Wang, G. Mapping forest ecosystem biomass density for Xiangjiang River Basin by combining plot and remote sensing data and comparing spatial extrapolation methods. *Remote Sens.* **2017**, *9*, 241. [CrossRef]
12. Li, L.; Zhou, X.; Chen, L.; Chen, L.; Zhang, Y.; Liu, Y. Estimating urban vegetation biomass from Sentinel- 2A image data. *Forest* **2020**, *11*, 125. [CrossRef]
13. Castillo-Santiago, M.Á.; Ghilardi, A.; Oyama, K.; Hernández-Stefanoni, J.L.; Torres, I.; Flamenco-Sandoval, A.; Fernández, A.; Mas, J.F. Estimating the spatial distribution of woody biomass suitable for charcoal making from remote sensing and geostatistics in central Mexico. *Energy Sustain. Dev.* **2013**, *17*, 177–188. [CrossRef]
14. Jubanski, J.; Ballhorn, U.; Kronseder, K.; Franke, J.; Siegert, F. Detection of large above-ground biomass variability in lowland forest ecosystems by airborne LiDAR. *Biogeosciences* **2013**, *10*, 3917–3930. [CrossRef]
15. Bazezew, M.N.; Hussin, Y.A.; Kloosterman, E.H. Integrating airborne LiDAR and terrestrial laser scanner forest parameters for accurate above-ground biomass/carbon estimation in Ayer Hitam tropical forest, Malaysia. *Int. J. Appl. Earth Obs. Geoinf.* **2018**, *73*, 638–652. [CrossRef]
16. Solberg, S.; Hansen, E.H.; Gobakken, T.; Næssset, E.; Zahabu, E. Biomass and InSAR height relationship in a dense tropical forest. *Remote Sens. Environ.* **2017**, *192*, 166–175. [CrossRef]
17. Schröter, M.; Remme, R.P.; Sumarga, E.; Barton, D.; Hein, L. Lessons learned for spatial modelling of ecosystem services in support of ecosystem accounting. *Ecosyst. Serv.* **2015**, *13*, 64–69. [CrossRef]
18. Su, Y.; Guo, Q.; Xue, B.; Hu, T.; Alvarez, O.; Tao, S.; Fang, J. Spatial distribution of forest aboveground biomass in China: Estimation through combination of spaceborne lidar, optical imagery, and forest inventory data. *Remote Sens. Environ.* **2016**, *173*, 187–199. [CrossRef]

19. Hlatshwayo, S.T.; Mutanga, O.; Lottering, R.T.; Kiala, Z.; Ismail, R. Mapping forest aboveground biomass in the reforested Buffelsdraai landfill site using texture combinations computed from SPOT-6 pan-sharpened imagery. *Int. J. Appl. Earth Obs. Geoinf.* **2019**, *74*, 65–77. [CrossRef]
20. Ketterings, Q.M.; Coe, R.; van Noordwijk, M.; Ambagau', Y.; Palm, C.A. Reducing uncertainty in the use of allometric biomass equations for predicting above-ground tree biomass in mixed secondary forests. *For. Ecol. Manag.* **2001**, *146*, 199–209. [CrossRef]
21. Aalde, H.; Gonzalez, P.; Gytarsky, M.; Krug, T.; Kurz, W.A.; Ogle, S.; Raison, J.; Schoene, D.; Ravindranath, N.H.; Elhassan, N.G.; et al. Chapter 4: Forest land. In 2006 IPCC Guidelines for National Greenhouse Gas Inventories. Available online: https://www.ipcc-nggip.iges.or.jp/public/2006gl/pdf/4_Volume4/V4_04_Ch4_Forest_Land.pdf (accessed on 25 January 2019).
22. Sya'bani, Z.S. Allometric Equations for Estimating above Ground Biomass of Pine Stand in Lawu Mountain. Bachelor's Thesis, Bogor Agricultural University, Bogor, Indonesia, 2017.
23. Adinugroho, W.C.; Sidiyasa, K. Model for estimating above ground biomass of mahogany tree. *J. Penelit. Hutan Dan Konserv. Alam* **2006**, *3*, 103–117. [CrossRef]
24. Alhamd, L.; Rahajoe, J.S. Species composition and above ground biomass of a pine forest at Bodogol, Gunung Gede Pangrango National Park, West Java. *J. Trop. Biol. Conserv.* **2013**, *10*, 43–49.
25. Malmoud, E. *Accuracy Measures and the Evaluation of Forecasts*; The University of Michigan: Ann Arbor, MI, USA, 1986.
26. R Core Team. *R: A Language and Environment for Statistical Computing. R Foundation for Statistical Computing*; R Core Team: Vienna, Austria, 2019.
27. Pebesma, E.J. Multivariable geostatistics in S: The gstat package. *Comput. Geosci.* **2004**, *30*, 683–691. [CrossRef]
28. Li, W.; Niu, Z.; Liang, X.; Li, Z.; Huang, N.; Gao, S.; Wang, C.; Muhammad, S. Geostatistical modeling using LiDAR-derived prior knowledge with SPOT-6 data to estimate temperate forest canopy cover and above-ground biomass via stratified random sampling. *Int. J. Appl. Earth Obs. Geoinf.* **2015**, *41*, 88–98. [CrossRef]
29. Spanò, M.; Leronni, V.; Lafortezza, R.; Gentile, F. Are ecosystem service hotspots located in protected areas? Results from a study in Southern Italy. *Environ. Sci. Policy* **2017**, *73*, 52–60. [CrossRef]
30. Castro, A.J.; Martín-López, B.; López, E.; Plieninger, T.; Alcaraz-Segura, D.; Vaughn, C.C.; Cabello, J. Do protected areas networks ensure the supply of ecosystem services? Spatial patterns of two nature reserve systems in semi-arid Spain. *Appl. Geogr.* **2015**, *60*, 1–9. [CrossRef]
31. Siregar, U.J.; Narendra, B.H.; Suryana, J.; Siregar, C.A.; Weston, C. Evaluation on community tree plantations as sustainable source for rural bioenergy in Indonesia. In Proceedings of the IOP Conference Series: Earth and Environmental Science, Bogor, Indonesia, 10–11 October 2016.
32. Masripatin, N.; Ginoga, K.; Pari, G.; Dharmawan, W.S.; Siregar, C.A. *Carbon Stocks on Various Types of Forest and Vegetation in Indonesia*; Forest Research and Development Agency, Ministry of Forestry of Indonesia: Jakarta, Indonesia, 2010.
33. Toma, T.; Ishida, A.; Matius, P. Long-term monitoring of post-fire aboveground biomass recovery in a lowland dipterocarp forest in East Kalimantan, Indonesia. *Nutr. Cycl. Agroecosyst.* **2005**, *71*, 63–72. [CrossRef]
34. Krisnawati, H.; Wahjono, D.; Imanuddin, R. Changes in the species composition, stand structure and aboveground biomass of a lowland dipterocarp forest in Samboja, East Kalimantan. *J. For. Res.* **2011**, *8*, 1–16. [CrossRef]
35. Waring, B.G.; Powers, J.F. Overlooking what is underground: Root:shoot ratios and coarse root allometric equations for tropical forests. *For. Ecol. Manag.* **2019**, *385*, 10–15. [CrossRef]
36. Medrilzam, M.; Dargusch, P.; Herbohn, J.; Smith, C. The socio-ecological drivers of forest degradation in part of the tropical peatlands of Central Kalimantan, Indonesia. *Forestry* **2013**, *87*, 335–345. [CrossRef]
37. Sumarga, E. Spatial indicators for human activities may explain the 2015 fire hotspot distribution in Central Kalimantan, Indonesia. *Trop. Conserv. Sci.* **2017**, *10*, 1940082917706168. [CrossRef]
38. Chen, X.; Liu, S.; Zhu, Z.; Vogelmann, J.; Li, Z.; Ohlen, D. Estimating aboveground forest biomass carbon and fire consumption in the U.S. Utah High Plateaus using data from the Forest Inventory and Analysis Program, Landsat, and LANDFIRE. *Ecol. Indic.* **2011**, *11*, 140–148. [CrossRef]
39. Wu, X.; Wang, S.; Fu, B.; Liu, Y.; Zhu, Y. Land use optimization based on ecosystem service assessment: A case study in the Yanhe watershed. *Land Use Policy* **2018**, *72*, 303–312. [CrossRef]

40. Sumarga, E.; Hein, L. Mapping ecosystem services for land use planning, the case of Central Kalimantan. *Environ. Manag.* **2014**, *54*, 84–97. [CrossRef] [PubMed]
41. Tammi, I.; Mustajärvi, K.; Rasinmäki, J. Integrating spatial valuation of ecosystem services into regional planning and development. *Ecosyst. Serv.* **2017**, *26 Pt B*, 329–344. [CrossRef]